Deuterium Isotope Effects on Rotation of Methyl Hydrogens. A Study of the Dimethyl Ether Radical Cation by ESR Spectroscopy and ab Initio and Density Functional Theory

Masaru Shiotani,*,† Nobuyuki Isamoto,† Michiro Hayashi,† Torbjörn Fängström,‡ and Sten Lunell*,‡

Contribution from the Department of Applied Chemistry, Faculty of Engineering, Hiroshima University, Higashi-Hiroshima 739, Japan, and Department of Quantum Chemistry, Uppsala University, Box 518, S-751 20 Uppsala, Sweden

Received March 30, 2000. Revised Manuscript Received September 5, 2000

Abstract: Deuterium isotope effects on the methyl group conformation and ESR spectra of selectively deuterated dimethyl ether radical cations are demonstrated by employing experimental matrix-isolation ESR techniques in combination with accurate ab initio and density functional theory (DFT) quantum chemical methods. The experimental study shows strong deuterium isotope effects on the proton hyperfine coupling constants (HFCC) for $CD_3OCH_3^+$, $CD_3OCH_2D^+$, and $CD_3OCHD_2^+$ as well as a temperature dependence in the HFCC for $CD_3OCH_2D^+$ and $CD_3OCHD_2^+$. The deuterium isotope effects and temperature dependencies can be understood by incorporating the mass difference of the two hydrogen isotopes in addition to their magnetic properties, and utilizing new, improved quantum chemical structure calculations. Good agreement between experiment and theory is obtained when correlated ab initio (MP2) geometries are used in conjunction with DFT hyperfine coupling constants, whereas an erroneous temperature behavior is obtained for the HFCC when older methods or DFT calculations are used for the geometry determinations.

1. Introduction

Use of selectively ^{2}D-labeled compounds has been found to be essential for an unequivocal assignment of electron spin resonance (ESR) spectra of organic radicals.[1−3]The great usefulness of ^{2}D labeling in this context is, as is well known, a consequence of the difference in magnetic properties between the proton and the deuteron. In certain cases, however, also the mass difference between these two hydrogen isotopes can affect the ESR spectrum significantly.[4−10] In the present theoretical and experimental study on selectively deuterated dimethyl ether radical cations, clear deuterium isotope effects on the methyl group conformation and ESR spectra are demonstrated, which can be shown to be caused by the above-mentioned mass difference.

Previous ESR experiments performed in a halocarbon matrix at 97 K on the dimethyl ether radical cation (DME^+) showed a spectrum consisting of seven lines with approximately binomial intensity ratios, indicating six equivalent protons in the radical.[11] These experiments were supported by a theoretical study in which the averaged isotropic hyperfine coupling constants (HFCC) of the three β protons were calculated to a value in close agreement with the experimental one.[12] The calculated structure of DME^+ reported by Momose et al.[12] exposed a symmetric structure with the two methyl groups occupying an eclipsed position relative to each other.

In the present matrix-isolation ESR study, the effect of selective deuteration of DME^+ is considered. The recorded ESR spectra show strong deuterium isotope effects for $CD_3OCH_3^+$, $CD_3OCH_2D^+$, and $CD_3OCHD_2^+$. The total ^{1}H HFCC of $CD_3OCH_3^+$ showed no significant temperature dependence in the temperature range of the experiments, 4.2−100 K, suggesting that the observed isotropic ^{1}H HFCC is rotationally averaged even at 4.2 K. Further deuteration of $CD_3OCH_3^+$, however, introduces a temperature dependency in the experimental HFCC for both $CD_3OCH_2D^+$ and $CD_3OCHD_2^+$. It will be shown below how these temperature dependencies can be understood by introducing the masses of the two hydrogen isotopes, in combination with new, improved structure determinations by accurate quantum chemical methods

2. Experimental Section

Samples and ESR Measurements. The dimethyl ether molecules used in the experiments are as follows: CH_3OCH_3

† Hiroshima University.
‡ Uppsala University.

(1) Shiotani, M. *Magn. Reson. Rev.* **1987**, *12*, 33.
(2) Shiotani, M.; Yoshida, H. ESR of radical ions. In *CRC Handbook of Radiation Chemistry*; Tabata, Y., Ed.; CRC Press: Boca Raton, FL, 1991; Chapter VIII.C.
(3) Lund, A., Shiotani, M., Eds. *Radical ionic systems: Properties in condensed phases*; Kluwer Academic Publishers, Dordrecht, The Netherlands,-1991.
(4) Lunell, S.; Eriksson, L. A.; Worstbrock, L. *J. Am. Chem. Soc.* **1991**, *113*, 7508.
(5) Knight, L. B.; Gregory, B. W.; Hill, D. W.; Arrington, C. A.; Momose, T.; Shida, T. *J. Chem. Phys.* **1991**, *94*, 67.
(6) Eriksson, L. A.; Lunell, S. *J. Am. Chem. Soc.* **1992**, *114*, 4532.
(7) Eriksson, L. A.; Lunell, S. *J. Am. Chem. Soc.* **1993**, *97:12*, 215.
(8) Matsushita, M.; Momose, T.; Shida, T.; Knight, L. B. *J. Chem. Phys.* **1995**, *103*, 3367.
(9) Knight, L. B.; King, G. M.; Petty, J. T.; Matsushita, M.; Momose, T.; Shida, T. *J. Chem. Phys.* **1995**, *103*, 3377.
(10) Wang, P.; Shiotani, M.; Lunell, S. *Chem. Phys. Lett.* **1998**, *292*, 110.
(11) Tzong, J.; Williams, F. *J. Am. Chem. Soc.* **1981**, *103*, 6994.
(12) Momose, T.; Nakatsuji, H.; Shida, T. *J. Chem Phys.* **1988**, *71*, 89.

10.1021/ja0011257 CCC: $19.00
Published on Web 11/18/2000

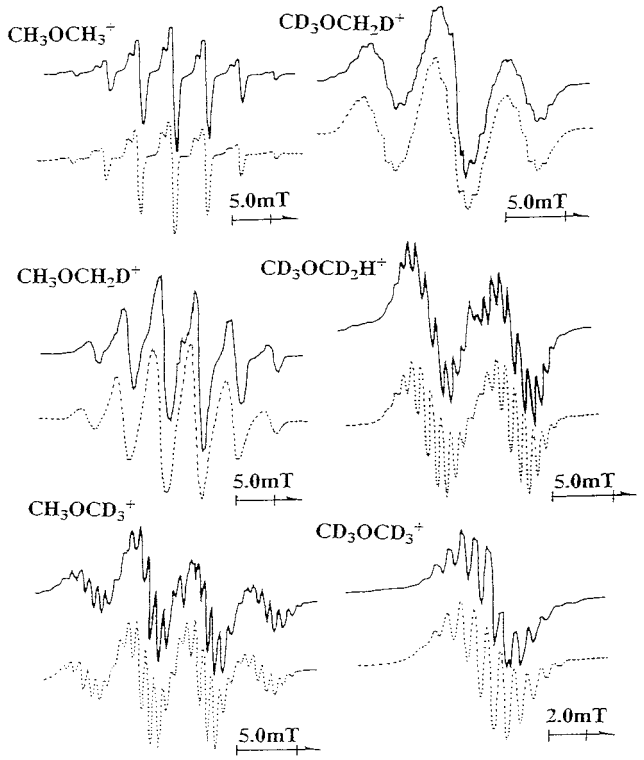

Figure 1. ESR spectra of six different ^{2}D-labeled dimethyl ether radical cations in CCl_3F at 77 K. The simulated spectra are shown with dotted lines.

(DME); CH_3OCH_2D (DME-d_1); CD_3OCH_3 (DME-d_3); CD_3OCH_2D (DME-d_4); CD_3OCHD_2 (DME-d_5); CD_3OCD_3 (DME-d_6).

Solid solutions containing ~1 mol % solute molecule in a halocarbon matrix were prepared in a Suprasil ESR sample tube, by several cycles of freezing, degassing, and thawing on a vacuum line. They were irradiated with γ-rays from ^{60}Co with a total dose of ~1 Mrad at 77 K and subjected to an ESR study. The method is well established to generate solute molecule radical cations and stabilize these in the matrix.[1−3]

The selectively deuterated dimethyl ethers (DME-d_n; n = 1−6) were synthesized by conventional methods (Williamson synthesis; see, for example, ref 13), and their purity was confirmed by the ^{1}H and ^{13}C NMR spectra (JEOL Ex-270 spectrometer). The substitution ratio of D to H at a certain position in the selectively deuterated compounds was 99%; the ratio is usually governed by the deuterium content of $LiAlD_4$ (Aldrich Chemical Co.) used as a reducing reagent. The matrix molecules used are halocarbons such as CCl_3F, CCl_2FCClF_2, CCl_3CF_3, $CClF_2CClF_2$, $CBrF_2CBrF_2$, cC_6F_{12}, and CF_3-cC_6F_{11}. They were used without further purification.

The ESR spectra were measured on a Bruker ESP 300E spectrometer from 4.2 K to the temperature at which all solute radicals decayed. The temperature was controlled with an Oxford continuous-flow cryostat, ESR 900.

Temperature-Dependent ESR Spectra. Figure 1 shows the ESR spectra of six different deuterium-labeled dimethyl ether radical cations which were generated by ionizing radiation and stabilized in a halocarbon matrix (CCl_3F) at 77 K. In the spectra of the radical cations of $CD_3OCH_3^+$, $CD_3OCH_2D^+$, and $CD_3OCHD_2^+$, the number of ^{1}H hyperfine lines decreases from 4 to 3 to 2, respectively. The ^{1}H HFCC was found to increase with increasing number of substituted deuteriums, from 4.3 mT for $CD_3OCH_3^+$ to 5.2 mT for $CD_3OCH_2D^+$, to 6.2 mT for $CD_3OCHD_2^+$ at 77 K (cf. Table 1).

(13) Morrison, R. T.; Boyd, R. N. *Organic Chemistry*, 6th ed.; Prentice Hall International: Upper Saddle River, NJ, 1992; p 241.

Table 1. Experimental ^{1}H and ^{2}D HFCCs of ^{2}D-Labeled Dimethyl Ether Radical Cations in a CCl_3F Matrix

radical	^{1}H hfsc and ^{2}D hfsc (mT)	T (K)
$CH_3OCH_3^+$	4.3 ($6H_\beta$)	10[a]
	4.3 ($6H_\beta$)	
$CH_3OCH_2D^+$	4.3 ($3H_\beta$), 5.2 ($2H_\beta$), 0.5 ($1D_\beta$)	77[a]
$CH_3OCD_3^+$	4.3 ($3H_\beta$), 0.6 ($3D_\beta$)	10[a]
	4.3 ($3H_\beta$), 0.6 ($3D_\beta$)	77[b]
$CD_3OCH_2D^+$	8.4 ($1H_\beta$), 4.2 ($1H_\beta$), 0.6 ($4D_\beta$)	4.2[a]
	5.2 ($2H_\beta$), 0.6 ($4D_\beta$)	77[b]
$CD_3OCHD_2^+$	8.8 ($1H_\beta$), 0.6 ($5D_\beta$)	10[a]
	6.2 ($1H_\beta$), 0.6 ($5D_\beta$)	77[b]
$CD_3OCD_3^+$	0.6 ($6D_\beta$)	77[b]

[a] In CCl_3F. [b] In all halocarbon matrixes used.

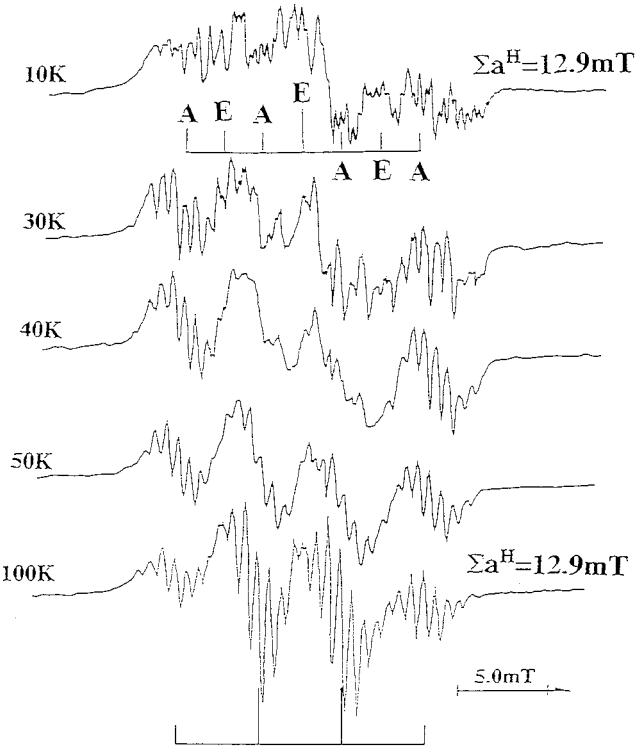

Figure 2. Temperature-dependent ESR spectra of $CD_3OCH_3^+$ in CCl_3F.

The radical cation of DME-d_1 gave a six-line spectrum whose ^{1}H HFCCs were 4.3 mT for the three equivalent CH_3 protons and 5.2 mT for the two equivalent CH_2D protons. This suggests that the deuterium substitution affects the ^{1}H HFCC of the hydrogen(s) belonging to the same methyl group, not that of the other methyl group. The ESR line-width was found to be too broad (~0.5 mT) to detect the corresponding shift in the ^{2}D HFCC. Similar ESR results were obtained by using the other halocarbons listed above as matrixes.

Temperature-dependent ESR spectra were observed for the radical cations in the temperature range from 4 to 100 K. At 100 K, the radical cations undergo changes to neutral radicals. Figure 2 shows the temperature-dependent ESR spectra of $CD_3OCH_3^+$ between 10 and 100 K. Although the HF patterns in the temperatures below 30 K are complicated because of overlapping with the smaller ^{2}D splittings of ~0.6 mT, due to"A-lines" and "E-lines", the latter, being characteristic of the tunneling rotation of the methyl hydrogens, are seen in the spectrum as observed for the DME radical cation.[12] No appreciable temperature dependence was observed for the ^{1}H

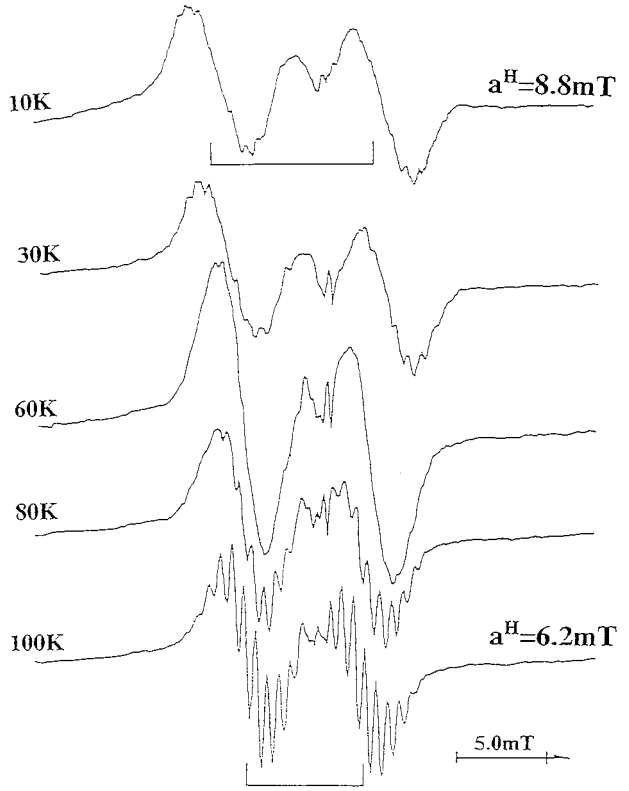

Figure 3. Temperature-dependent ESR spectra of $CD_3OCHD_2^+$ in CCl_3F.

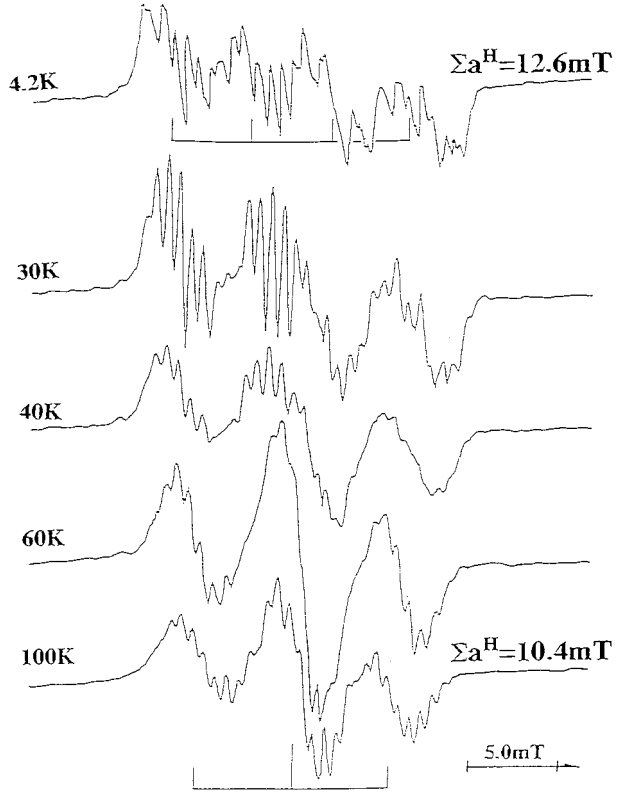

Figure 4. Temperature-dependent ESR spectra of $CD_3OCH_2D^+$ in CCl_3F.

HFCC of the CH_3 group, which indicates that the HFCC of 4.3 mT corresponds to the rotationally averaged value of $CH_3OCH_3^+$. On the other hand, it was found that the ^{1}H HFCC of $CD_3OCHD_2^+$ decreases with increasing temperature from 8.8 mT at 4 K to 6.2 mT at 80 K. Above 80 K, the HFCC becomes almost constant up to 100 K (cf. Figures 3 and 7).

These results lead us to the conclusion that the light hydrogen of the CHD_2 group in $CD_3OCHD_2^+$ takes a fixed position at 4 K and that the light and heavy hydrogens (^{1}H and ^{2}D) cannot be completely averaged out even at the higher temperature of 100 K. Using a McConnell type of equation for the β-proton, $a_H^\beta = B_0 \cos^2\theta$,[14] and the experimental HFCC of 4.3 mT for the rotational averaging, $\langle a_H^\beta \rangle = 4.3$ mT, we have 8.6 mT for the proportionality constant, B_0. Comparing with the experimental value of 8.8 mT for the ^{1}H HFCC of CHD_2 at 4.2 K, we can conclude that the light hydrogen (^{1}H) selectively occupies a position close to $\theta = 0°$, which is parallel to the unpaired p-orbital of the oxygen atom.

The preference of the light hydrogen to occupy the $\theta \simeq 0°$ position can be qualitatively explained by hyperconjugation. Through this effect, which is a maximum around this position, the singly occupied molecular orbital (SOMO) will be delocalized from oxygen to hydrogen making the corresponding C−H bond weaker and longer. Since the zero-point vibrational energy (ZPE) of a C−H stretching vibration to a first approximation is proportional to $(k/m)^{1/2}$, k being the force constant and m the mass of the hydrogen nucleus, the decrease in the ZPE upon deuteration will be larger for bonds having higher force constants. The deuterium atoms will hence preferentially occupy sites with larger force constants, leaving the $\theta \simeq 0°$ position to the light hydrogen. Similar deuterium effects on the methyl hydrogen conformation have been reported for the partially deuterated monofluoromethane radical cation of $CFDH_2^+$ by Knight et al.[5]

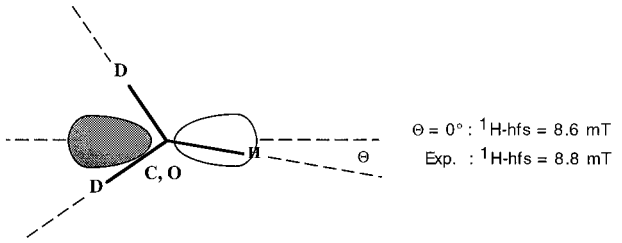

A similar temperature dependence was also observed for the ^{1}H HFCC of $CD_3OCH_2D^+$, as shown in Figure 4: the total HFCC of the spectrum decreases from 12.6 (4.2 K) to 10.4 mT (100 K). Although the 4.2 K spectrum is rather complex, the main spectral feature can be seen to consist of four hf lines due to two nonequivalent protons with ∼8.4 and ∼4.2 mT.

The ESR spectrum of $CH_3OCH_3^+$ in a $CF_2ClCFCl_2$ matrix was irreversibly changed into a binomial triplet with ^{1}H HFCC of 2.0 mT upon warming above 100 K. The spectrum can be assigned to a neutral radical having two equivalent α-hydrogens, i.e., $^\bullet CH_2OCH_3$. The radical cation of $CH_3OCD_3^+$ was found to be converted into $^\bullet CH_2OCD_3$ and $CH_3OCD_2^\bullet$ with equal yields. Thus, no deuterium effects was observed for the deprotonation reaction of the dimethyl ether radical cations.

We summarize the present experimental results as follows:

1. Strong and very clear deuterium isotope effects (mass effects) were observed for conformation and rotation of the methyl hydrogens of selectively deuterated dimethyl ether radical cations: $CD_3OCHD_2^+$, $CD_3OCDH_2^+$, $CD_3OCH_3^+$, etc.
2. $CD_3OCHD_2^+$ gives a large ^{1}H HFCC of 8.8 mT at 4 K.
3. The results suggest that the light hydrogen preferentially occupies a position closely parallel to the unpaired p-orbital of the oxygen atom.

(14) Carrington, A.; McLachlan, A. D. *Introduction to Magnetic Resonance*; Harper & Row: New York, 1967.

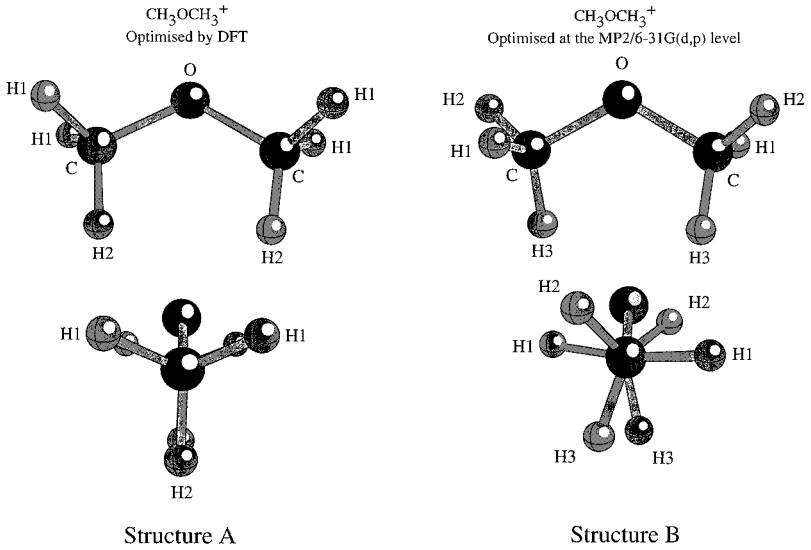

Figure 5. Optimized structure of $CD_3OCH_3^+$, obtained using the DFT and MP2 methods, respectively (cf. Table 3).

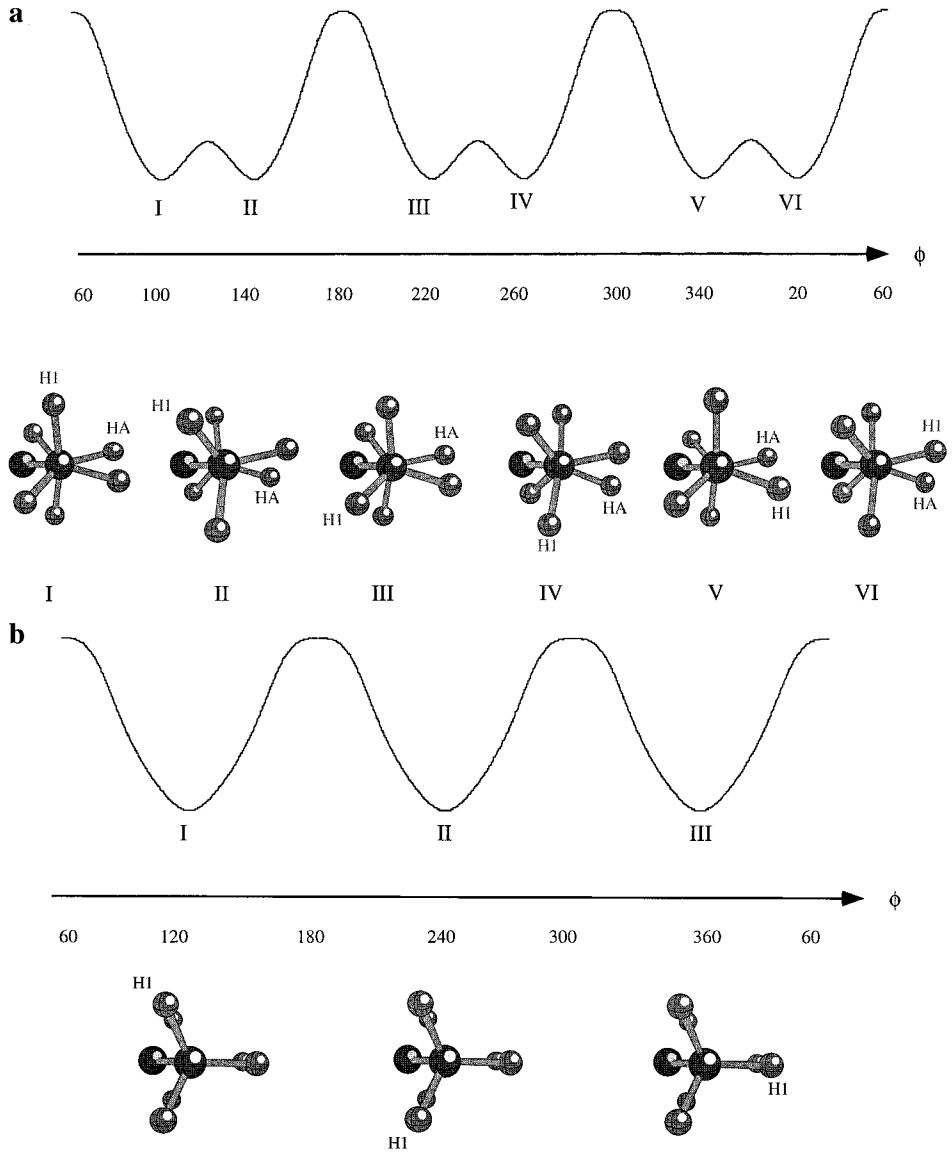

Figure 6. (a) Rotational barriers for CH_3 rotation, calculated by the MP2/6-31G(d,p) method. Indicated in the picture is the rotational angle, ϕ, defined as the angle between the C−O−C and H1−O−C planes. (b) Rotational barriers for CH_3 rotation, calculated by B3LYP/6-31G(d,p).

4. The ^{1}H HFCC decreases with increasing temperature from 8.8 (4.2 K) to 6.2 mT (80 K), but an complete exchange between ^{1}H and ^{2}D of the CHD_2 group does not occur. The reason for this is discussed in detail in section 4.

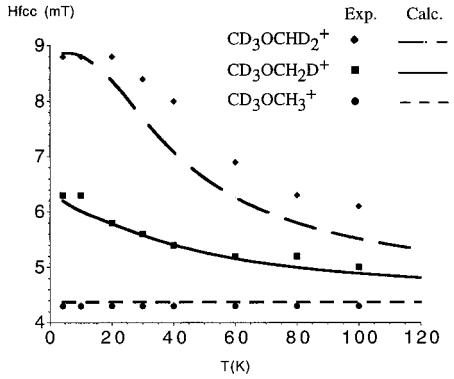

Figure 7. Experimental and BLYP/6-311+G(2df,p)/MP2/6-31G(d,p) calculated ^{1}H HFCC as functions of temperature (cf. Table 6).

3. Theoretical Section

3.1. Methods. If a molecule can exist in several forms, for example, rotational or cis and trans isomers, and the forms are interchanging rapidly (i.e., the case in which the interchange rate is much larger than the difference between the associated HFCCs) a mean HFCC will be obtained as

$$\langle a \rangle = p_{\mathrm{I}} a_{\mathrm{I}} + p_{\mathrm{II}} a_{\mathrm{II}} + p_{\mathrm{III}} a_{\mathrm{III}} \cdots \quad (1)$$

where p_{I}, p_{II}, p_{III}, ... are the probabilities of finding the different forms and a_{I}, a_{II}, ... are the corresponding HFCCs.[15] As already mentioned, the deuterium atoms in partially deuterated methyl groups will preferentially occupy sites with larger C−H force constants, to minimize the ZPE. Changing the level of deuteration and/or changing the sites that the deuterium atoms occupy will affect the ZPE. Accordingly, different rotational isomers of DME^+ will have different ZPE depending both on how many sites that are occupied by deuterium atoms and on their position. At higher temperatures, also such rotational isomers where the deuterons occupy less favorable sites will obtain a nonzero probability. Assuming that the different rotational isomers are populated with probabilities determined by a Boltzmann distribution, a dependency both on the temperature and on the level of deuteration is hence obtained in the calculated HFCC values. This model for the temperature dependency in the HFCC will be used to analyze the experimental results presented in the previous section.

Geometry optimizations were performed at correlated ab initio and density functional theory (DFT) levels for the ground state of the dimethyl ether radical cation (DME^+). In the ab initio calculations, electron correlation was included through Møller−Plesset perturbation theory[16] to second order (MP2). For all geometry optimizations and energy calculations at the MP2 level, the frozen core approximation was employed. Three different functionals were used in the DFT calculations, referred to as B3LYP, BLYP, and BP86, respectively. The B3LYP functional is based on Becke's three-parameter adiabatic connection method (ACM) approach and consists of a combination of Slater,[17] Hartree−Fock,[18] and Becke[19] exchange and the Vosko, Wilk, and Nusair (VWN) local[20] and Lee, Yang, and Parr (LYP)[21] nonlocal correlation functional. The BLYP functional is built from the nonlocal exchange functional by Becke,[19] the VWN local correlation functional, and the nonlocal LYP correlation functional. The BP86 functional, finally, has the same exchange part as in BLYP, together with Perdew's gradient-corrected correlation functional.[22] Two basis sets, the 6-31G(d,p)[23,24] and 6-311+G(d,p),[25,26] were used in all ab initio and DFT optimizations. To get more reliable values of the energies for the different stationary points on the MP2 potential energy surfaces (PES), a number of single-point calculations using MP4(SDTQ)/6-31G(d,p)[27] were performed. Isotropic HFCCs for the hydrogens are reported for the stationary points found both at the different DFT levels and at the MP2 level of approximation. Results for the HFCC are presented from the B3LYP, BLYP, and BP86 calculations using the 6-31G(d,p) and 6-311+G(2df,p)[25,26,28−30] bases.

Frequency calculations were performed at the MP2/6-31G(d,p) and B3LYP/6-31G(d,p) levels for different rotational isomers of $CH_3OCH_2D^+$ and $CH_3OCHD_2^+$ to estimate the change in ZPE due to deuteration at different sites.

Table 2. DFT/6-31G(d,p) and DFT/6-311+G(d,p) Optimized Structures for $CH_3OCH_3^+$[a]

method	B3LYP	BLYP	BP86
R(C−O)	1.407 (1.410)[b]	1.419 (1.422)	1.407 (1.411)
R(C−H1)	1.105 (1.106)	1.114 (1.115)	1.117 (1.117)
R(C−H2)	1.088 (1.089)	1.094 (1.100)	1.097 (1.099)
∠(C−O−C)	121.96 (121.85)	121.52 (121.30)	121.11 (121.02)

[a] Distances in angstroms and angles in degrees. The three functionals B3LYP, BLYP, and BP86 were used in the DFT calculations. [b] The values in parentheses were obtained using the smaller 6-31G(d,p) basis.

3.2. Structure of $CH_3OCH_3^+$ at the DFT and the MP2 Levels of Approximation. Geometry optimizations at DFT levels of theory result in one energy minimum structure, similar to the one reported by Momose et al.[12] (cf. Figure 5). The structure shows two groups of hydrogens, one with four equivalent hydrogens (H1) and one with two equivalent hydrogens (H2). Only minor changes in the structure are seen upon changing the functional or basis. The largest difference in bond lengths between the three functionals used is not more than 0.012 Å, the differences in bond angles are at most 1°, and the difference in the CH_3 torsional angle is at most 0.6°. When the basis is increased from 6-31G(d,p) to 6-311+G(d,p), the geometrical changes are even smaller compared to the changes seen upon changing the functional (cf. Table 2). Performing a frequency calculation, the structure found at the B3LYP/6-31G(d,p) level was verified to be a true energy minimum at this level of calculation.

Due to the very similar results for the functionals and basis sets used, frequency calculations were only performed at the B3LYP/6-31G(d,p) level among the DFT methods.

In contrast to the DFT methods, optimizations at the MP2/6-31G(d,p) level of theory yield two types of energy extremes, one of which is similar in shape to the ones found at the DFT

(15) Fraenkel, G. *J. Phys. Chem.* **1967**, *71*, 139.
(16) Møller, C.; Plesset, M. S. *Phys. Rev.* 1934, 46, 618.
(17) Slater, J. C. *Quantum Theory of Molecules and Solids. The Self-Consistent Field for Molecules and Solids*; McGraw-Hill: New York, 1974; Vol. 4.
(18) Fock, V. *Z. Phys.* **1930**, *61*, 126.
(19) Becke, A. D. *Phys. Rev.* **1988**, *38*, 3098.
(20) Vosko, S. H.; Wilk, L.; Nusair, M. *Can. J. Phys.* **1980**, *58*, 1200.
(21) Lee, C.; Yang, W.; Parr, R. G. *Phys. Rev. B* **1988**, *37*, 785.
(22) Perdew, J. P. *Phys. Rev. B.* **1986**, *33*, 8822.
(23) Hariharan, P. C.; Pople, J. A. *Theor. Chim. Acta* **1973**, *28*, 213.
(24) Francl, M. M.; Petro, W. J.; Hehre, W. J.; Binkley, J. S.; Gordon, M. S.; DeFrees, D. J.; Pople, J. A. *J. Chem. Phys.* **1982**, *77*, 3654.
(25) Krishnan, R.; Binkley, J. S.; Seeger, R.; Pople, J. A. *J. Chem. Phys.* **1980**, *72*, 650.
(26) Clark, T.; Chandrasekhar, J.; Spitznagel, G. W.; Schleyer, P. von R. *J. Comput. Chem.* **1983**, *4*, 294.
(27) Krishnan, R.; Pople, J. A. *Int. J. Quant. Chem.* **1978**, *14*, 91.
(28) McLean, A. D.; Chandler, G. S. *J. Chem. Phys.* **1980**, *72*, 5639.
(29) Gill, P. M. W.; Johnson, B. G.; Pople, J. A.; Frisch, M. *J. Chem, Phys. Lett.* **1992**, *197*, 499.
(30) Frisch, M. J.; Pople, J. A.; Binkley, J. S.; Schleyer, P. v. R. *J. Chem. Phys.* **1984**, *80*, 3265.

levels (structure A) and one slightly different structure with three unequal C−H bonds (structure B), giving rise to three groups of pairwise equivalent hydrogen atoms (H1, H2, and H3); cf. Figure 5 and Table 3. The energy of structure A is 0.6 kJ/mol less stable compared to structure B both at the MP2/6-31G-(d,p) and at the MP4/6-31G(d,p) levels. Moreover, in the frequency calculations, structure A exposes one imaginary frequency and is predicted to be a transition state at this level of theory. Structure B showed only real frequencies in the calculation. When the basis set was increased from 6-31G(d,p) to 6-311+G(d,p), the changes in bond lengths and bond angles were less than 0.01 Å and 1°, respectively. A somewhat larger change of at most 3.5° was observed in the CH_3 torsional angle.

3.3. Potential Energy Surface for the Methyl Group Rotation. Inspired by the above results concerning the energy minimum structures at the MP2 and the DFT levels, a more careful investigation of the PES for the methyl group rotation was performed at the MP2/6-31G(d,p) level of theory. A rotational angle, defined as the angle between the C,O,C and the H1,O,C planes, was used as the governing variable for the rotation. A sequence of calculations was performed, keeping the governing variable fix and optimizing all other variables in each step. Two energy barriers in the PES scan of the methyl group, one small (0.3 kJ/mol) and one somewhat larger (1.3 kJ/mol), were found at the MP2/6-31G(d,p) level of theory. For each rotational energy minimum there exist two energetically favorable positions of the second methyl group at the MP2 level; cf. Figure 6a. Hence for a full turn of the methyl group there are six rotational minimums at the MP2 level.

The splitting of each of the 3-fold minimums into two minimums separated by a low barrier can be seen as a result of a gearing between the rotations of the two methyl groups, which hence cannot be considered as two independent rotors. It is in this connection interesting to note that a careful investigation of the infrared spectrum of neutral DME[31] clearly has demonstrated the necessity of including simultaneously both gearing and bending modes for a satisfactory analysis of the torsional band spectrum. The appearance of terms dependent on cos 6θ, and not only cos 3θ, in potentials governing methyl group rotation, has been documented in connection with other spectroscopies on neutral molecules, e.g., neutron scattering, microwave, and optical spectroscopy.[32−34]

At the DFT level, all our attempts to find a second stationary point with the methyl groups offset from an eclipsed position relative to each other failed, independent of functional or basis set. The rotational energy profile at the DFT levels of approximation was hence found to contain only three rotational minimums for a full turn of the methyl group; cf. Figure 6b. The value of the energy barrier in the PES scan of the methyl group was 2.9 kJ/mol at the B3LYP/6-31G(d,p) level, a somewhat larger value compared to the one at the MP2/6-31G-(d,p) level.

4. Discussion

Due to the very small changes observed in geometry upon enlargement of the basis set (cf. Tables 2 and 3), the geometry obtained with the smaller basis is used in the following discussion concerning the HFCC. The average of the three methyl protons HFCC, using the MP2 geometry is calculated to lie between 4.0 (B3LYP/6-311+G(2df,p)//MP2/6-31G(d,p)) and 4.37 mT (BLYP/6-311+G(2df,p)//MP2/6-31G(d,p)). Using the DFT structure, somewhat larger average values are obtained, 4.38 (B3LYP/6-31G(d,p)//B3LYP/6-31G(d,p) to 4.72 mT (BLYP/6-311+G(2df,p)//BLYP/6-311+G(d,p)). All calculated values are in good agreement with the experimental value of 4.3 mT[11] (cf. Table 4).

Table 3. MP2/6-31G(d,p) and MP2/6-311+G(d,p) Optimized Structures and Relative Energies (in kJ/mol) for $CH_3OCH_3^+$[a]

	structure A	structure B
R(C−O)	1.414 (1.423)[b]	1.416 (1.424)
R(C−H1)	1.100 (1.094)	1.106 (1.100)
R(C−H2)	1.088 (1.083)	1.090 (1.088)
R(C−H3)		1.085 (1.085)
∠(C−O−C)	120.83 (121.18)	119.46 (120.07)
relative energy (MP2)	0.607 (0.297)	0 (0)
relative energy (MP4)	0.350	0

[a] The DFT and MP2 structures in Figure 5 correspond to structures A and B in the table, respectively. [b] The values in parentheses were obtained using the smaller 6-31G(d,p) basis.

The temperature-dependent HFCCs are calculated according to eq 1, using a Boltzmann distribution to calculate the probability to find the different rotational isomers. The ZPE are obtained from the frequency calculations at both the B3LYP/6-31G(d,p) and MP2/6−31(d,p) levels for $CD_3OCH_2D^+$ and $CD_3OCHD_2^+$ (cf. Table 5).

As can be seen, reasonable agreement between calculated and experimental values is obtained at all temperatures for the $CD_3OCH_2D^+$ isomer, using both the MP2 and the B3LYP geometries (cf. Table 6). The HFCCs used when calculating the mean HFCC according to eq 1 were obtained at the BLYP/6-311+G-(2df,p) level for the MP2 calculated structure (cf. Table 4; H1, 8.86 mT; H2, 3.57 mT; H3, 0.69 mT) and at the B3LYP/6-311+G(2df,p) level for the B3LYP calculated structure (cf. Table 4; H1, 6.63 mT; H2, −0.16 mT).

The situation for $CD_3OCHD_2^+$ is, however, quite different. In this case, the temperature dependence of the HFCC predicted using the DFT geometries differs considerably from the experimental one, especially for low temperatures (cf. Table 6), while the values calculated using the MP2/6-31G(d,p) geometries, on the other hand, fit nicely also for the $CD_3OCHD_2^+$ isomer (cf. Figure 7 and Table 6). Equilibrium structures at the MP2/6-31G(d,p) level with HFCCs calculated at the DFT level thus give good agreement with experiment for all isomers in the temperature interval of the experiment.

The calculated HFCCs obtained for the MP2 geometry also fit much better with the low-temperature (4.2 K) experimental values for $CD_3OCH_2D^+$ than the HFCCs obtained for the DFT geometry. In the static approximation, assuming the deuterium atom to occupy the site with the shortest C−H bond length, the calculated HFCCs that fit best the experimental ones are 8.86 and 3.57 mT (BLYP/6-311+G(2df,p)//MP2/6-31G(d,p) to be compared with the experimental values of 8.4 and 4.2 mT (cf. section 3).

To summarize the above discussion, the following explanation of the observed temperature-dependent ^{1}H HFCC for the different deuterated isomers emerges:

1. $CD_3OCHD_2^+$: The rotational isomer with the proton occupying the site with the longest C−H bond (corresponding to H1) will be the most stable rotational isomer, having the lowest ZPE, and the CHD_2 group is locked at 4 K in this energy minimum (cf, Figure 6a). This corresponds to the situation with θ close to =0° in a McConnell type of equation (cf. section 3).

(31) Senent, M. L.; Moule, D. C.; Smeyers, Y. G. *J. Chem. Phys.* **1995**, *102*, 5952.
(32) Cavagnat, D.; Brom, H.; Nugteren, P. R. *J. Chem. Phys.* **1987**, *87*, 901.
(33) Gorse, D.; Cavagnat, D.; Pesquer, M.; Lapouge, C. *J. Phys. Chem.* **1993**, *97*, 4262.
(34) Siebrand, W.; Zgierski, M. Z.; Zerbetto, F.; Lim, E. C. *J. Chem. Phys.* **1992**, *96*, 7973.

Table 4. Hydrogen HFCC (in mT) for Structures Optimized at the MP2 and DFT Levels Employing the 6-31G(d,p) and 6-311+G(d,p) Basis[a]

	method		
hydrogen	B3LYP/6-31G(d,p) //MP2/6-31G(d,p)	BLYP/6-31G(d,p) //MP2/6-31G(d,p)	BP86/6-31G(d,p) //MP26-31G(d,p)
H1	8.16	8.75	8.42
H2	3.25	3.51	3.38
H3	0.063	0.66	0.63
	method		
hydrogen	B3LYP/6-311+G(2df,p) //MP2/6-31G(d,p)	BLYP/6-311+G(2df,p) //MP2/6-31G(d,p)	BP86/6-311+G(2df,p) //MP2/6-31G(d,p)
H1	8.12	8.86	8.39
H2	3.24	3.57	3.38
H3	0.65	0.69	0.65
	method		
hydrogen	B3LYP/6-311+G(2df,p) //MP2/6-311G+(d,p)	BLYP/6-311G+(2df,p) //MP2/6-311G+(d,p)	BP86/6-311G+(2df,p) //MP2/6-311G+(d,p)
H1	8.85	9.25	8.76
H2	2.85	3.12	2.95
H3	0.95	1.02	0.96
	method		
hydrogen	B3LYP/6-31G(d,p) //B3LYP/6-31G(d,p)	BLYP/6-31G(d,p) //BLP/6-31G(d,p)	BP86/6-31G(d,p) //BP86-31G(d,p)
H1	6.65	7.00	6.89
H2	−0.17	−0.20	−0.21
	method		
hydrogen	B3LYP/6-311G+(2df,p) //B3LYP/6-31G(d,p)	BLYP/6-311G+(2df,p) //BLYP/6-31G(d,p)	BP86/6-311G+(2df,p) //BP86-31G(d,p)
H1	6.63	7.06	6.84
H2	−0.16	−0.19	−0.19
	method		
hydrogen	B3LYP/6-311+G(2df,p) //B3LYP/6-311+G(d,p)	BLYP/6-311+G(2df,p) //BLYP2/6-311+G(d,p)	BP86/6-311+G(2df,p) //BP86-311+G(d,p)
H1	6.72	7.12	6.90
H2	−0.16	−0.19	−0.19

[a] The values of the HFCC for the MP2 structure are obtained from single-point DFT calculations. For the numbering of the hydrogens, see Figure 5.

Table 5. Calculated (MP2/6-31G (d,p) and DFT/6-31G(d,p)) Zero-Point Vibrational Energies for the Different Rotational Isomers of $CD_3OCH_2D^+$ and $CD_3OCHD_2^+$

MP2/6-31G(d,p)		
	undeuterated positions	ZPE (kJ/mol)
$CD_3OCH_2D^+$	H1, H2	154.775
	H1, H3	154.943
	H2, H3	155.439
$CD_3OCHD_2^+$	H1	147.012
	H2	147.487
	H3	147.644
B3LYP/6-31G(d,p)		
$CD_3OCH_2D^+$	H1, H2	149.754
	H1, H1	149.165
$CD_3OCHD_2^+$	H1	142.024
	H2	142.584

2. $CD_3OCH_2D^+$: The rotational isomer with the deuterium atom occupying the site with the shortest bond (corresponding to the H3 position) has the lowest ZPE (cf. Table 5). The CH_2D group has two local energy minimums with identical ZPE and Boltzmann factors separated by the lower energy barrier (cf. Figure 6a). An oscillation between these minimums corresponds to an exchange of the H1 and H2 positions, while not affecting H3. A rotation of the CH_2D group to a position in which the deuterium atom occupies the H1 or the H2 position, in contrast, increases the ZPE, decreasing the probability for the protons to occupy the H3 position at low temperatures.

Table 6. Experimental and Calculated ^{1}H hfs Splittings (in mT) of ^{2}D-Labeled Dimethyl Ether Radical Cations in CCl_3F at Different Temperatures

	$CD_3OCDH_2^+$								
temperature (K)	10	20	30	40	50	60	77	80	100
BLYP//MP2[a]	6.05	5.78	5.57	5.40	5.26	5.15	5.01	4.99	4.89
B3LYP//B3LYP[b]	6.65	6.47	6.12	5.79	5.55	5.36	5.15	5.12	4.97
exp[c]	6.3	5.7	5.6	5.4		5.2	5.2		5.0
	$CD_3OCD_2H^+$								
temperature (K)	10	20	30	40	50	60	77	80	100
BLYP/MP2a	8.84	8.41	7.69	7.06	6.60	6.25	5.85	5.79	5.51
B3LYP/B3LYP[b]	6.66	6.55	6.32	6.08	5.88	5.71	5.49	5.45	5.27
exp	8.8	8.8	8.4	8.0		6.9	6.2		6.1

[a] BLYP/6-311+G(2df,p)//MP2/6-31G(d,p). [b] B3LYP/6-311+G(2df,p)//B3LYP/6-31G(d,p). [c] Averaged value of the two protons.

The exchange rate of the two protons at the H1 and H2 positions is too low to completely average the associated ^{1}H HFCCs at low temperatures. However, above 30 K, the ^{1}H HFCC starts to be averaged, with the deuterium HFCC (at the H3 position) is unchanged.

3. $CD_3OCH_3^+$: All rotational isomers have the same probability according to eq 1, and a temperature-independent ^1H HFCC average is observed.

According to the above discussion, the main reason for certain rotamers of $CD_3OCH_2D^+$ and $CD_3OCD_2H^+$ to be unaccessed at low temperatures is not high potential barriers preventing the rotation, but rather the difference in ZPE for the different rotational isomers. From a computational point of view, very accurate barriers toward rotation may hence be less crucial than an accurate prediction of the equilibrium geometry and ZPE of the ground state.

The present experimental as well as theoretical results show that a strong influencing factor on the geometry of the DME^+ radical cation is the hyperconjugative interaction between the methyl groups and the oxygen p-orbital, which favors a torsion angle θ close to 0°, i.e., an eclipsed configuration of the two methyl groups (cf. section 3). This influence is, however, partially counteracted by the nonbonding, repulsive interaction between the C−H bonds, which offsets the equilibrium from the perfectly eclipsed conformation (cf. Figure 6a). As shown in section 4, available DFT methods apparently have not yet reached a level of sophistication that is sufficient to adequately describe these subtle effects of electron correlation. One conclusion of the present work is thus that correlated ab initio methods at the MP2 level or higher are needed for a satisfactory description of the nonbonding interactions between methyl groups separated by one (or more) atoms.

Effects of partial deuteration were studied also in some of the papers on neutral molecules mentioned in section 3.3.[32−34] In the present study, these effects can essentially be related to the changes in the strengths of the different carbon−hydrogen bonds introduced by the ionization. In the neutral molecules, the carbon−hydrogen bonds are much more similar, and accordingly, the differences in zero-point energies for the different rotamers are not as pronounced as in the present study. Nevertheless, it was found in the case of neutral nitromethane that the ZPE differences between different rotational conformers were sufficient to make them spectroscopically observable despite very low barriers to rotation.[33] A similar conclusion was reached also by Siebrand and co-workers[34] in the case of partially deuterated acetophenone. The present study shows that these phenomena can be observed also in ionized molecules and have a decisive influence on their ESR spectra at low temperatures.

Acknowledgment. This work was supported by the Swedish Natural Sciences Research Council (NFR). Grants of computer time on the IBM SP at the Center for Parallel Computers (PDC) in Stockholm and the Cray C90 of the Swedish Supercomputer Center (NSC) in Linköping are gratefully acknowledged. The present study was also supported by a Subsidy of Science Research of the Japanese Ministry of Education.

JA0011257